Catalysis Science & Technology

PAPER

View Article Online
View Journal | View Issue

Cite this: *Catal. Sci. Technol.*, 2016, **6**, 6853

Support effect for nanosized Au catalysts in hydrogen production from formic acid decomposition

Monika Zacharska,[ab] Andrey L. Chuvilin,[cd] Vladimir V. Kriventsov,[e] Sergey Beloshapkin,[b] Miguel Estrada,[f] Andrey Simakov[f] and Dmitri A. Bulushev*[egh]

Received 12th March 2016,
Accepted 6th May 2016

DOI: 10.1039/c6cy00552g

www.rsc.org/catalysis

Catalysts with about 2.5 wt% of gold supported on Al_2O_3, ZrO_2, CeO_2, La_2O_3 and MgO oxides and with the same mean metal particle sizes of 2.4–3.0 nm have been studied in hydrogen production *via* formic acid decomposition. A strong volcano-type relation of the catalytic activity on the electronegativity of the support's cation was demonstrated with the Au/Al_2O_3 catalyst on the top. This indicated that the activity is affected by the acid–base properties of the support. A study of the most active Au/Al_2O_3 catalyst with aberration-corrected HAADF/STEM, XPS and EXAFS proved that gold is in metallic state. The content of single supported gold atoms/cations was negligible. Therefore, the mechanism of the reaction was related to the activation of formic acid on the catalyst's support followed by further decomposition of the formed reaction intermediate on the Au/support interface.

Introduction

Biomass-derived formic acid containing 4.4 wt% of hydrogen is considered as a potential hydrogen source producing hydrogen by decomposition at low temperatures using noble metal catalysts.[1] This feature could be utilized further for important application of this acid in some hydrogenation reactions instead of molecular hydrogen[2,3] thus avoiding the problems of expensive hydrogen transportation. Heterogeneous catalysts could be used for decomposition of formic acid in liquid or vapour phase. In the present paper, we consider only vapour phase formic acid decomposition and gold catalysts on different supports.

Catalysis with nanosized gold has attracted a lot of attention during the last 15 years as gold catalysts with particle sizes smaller than 5 nm may provide a better performance in reactions where Pt-group metals are traditionally used. Thus, for formic acid decomposition, Ojeda and Iglesia[4] have demonstrated that the activity of Au/Al_2O_3 catalysts with a mean size of 2–4 nm could be one order of magnitude higher than that of Pt/Al_2O_3 catalysts. They assigned the exceptional activity to the presence of sub-nanometre sized Au species invisible by conventional TEM. However, these authors provided no spectroscopic or electron microscopy evidence of the presence of such species. The content of CO in these studies was less than 10 ppm, and hence, the reaction corresponded to CO-free hydrogen production. The explanation of these authors was based on the approach developed by the group of Flytzani-Stephanopoulos,[5] who demonstrated a unique activity of isolated $Au–O_x(OH)–$ species attached to reducible CeO_2, TiO_2 and Fe_2O_3 supports in water-gas shift (WGS) reaction. This group confirmed the presence of Au species in isolated atomic state in their catalysts by aberration-corrected HAADF/STEM studies. Later, they also investigated formic acid decomposition and showed that Au/CeO_2 catalysts containing only single Au atoms at low concentrations (0.03 and 0.5 at%), left on the support after leaching of Au nanoparticles by a NaCN solution, provided a catalytic activity towards H_2 and CO_2 products at low temperatures (<323 K).[6] These results were in accordance with the results of Ciftci *et al.*,[7] who used quite similar catalysts.

Alternatively, Singh *et al.*[8] using microkinetic modelling and density functional theory (DFT) calculations showed that the reaction of formic acid decomposition is structure-sensitive and the reaction rates are determined by a mechanism taking place *via* formate species decomposition over low coordinated corner sites located on the Au nanoparticles. They used an unreducible catalyst support (SiC), for which stabilization of single Au atoms is not expected, and the

[a] *Chemical & Environmental Sciences Department, University of Limerick, Limerick, Ireland*
[b] *Materials & Surface Science Institute, University of Limerick, Limerick, Ireland*
[c] *CIC nanoGUNE Consolider, Donostia - San Sebastián, 20018 Spain*
[d] *IKERBASQUE, Basque Foundation for Science, Bilbao, 20013 Spain*
[e] *Boreskov Institute of Catalysis, SB RAS, Novosibirsk 630090, Russia. E-mail: dmitri.bulushev@catalysis.ru*
[f] *Centro de Nanociencias y Nanotecnología de la UNAM, 22860, Ensenada, BC, México*
[g] *Novosibirsk State University, Novosibirsk 630090, Russia*
[h] *Nikolaev Institute of Inorganic Chemistry, SB RAS, Novosibirsk 630090, Russia*

mean Au particle sizes of their catalysts were in the range from 2.5 to 11 nm. The content of CO in these studies was negligible (~25 ppm).

Gazsi *et al.*[9] determined the catalytic activity in formic acid decomposition of 1 wt% Au catalysts on different supports. Comparing the activity of the catalysts with similar mean particle sizes of 5.5–6.5 nm at 473 K, they showed that an Au/SiO_2 catalyst demonstrated a 4–6 times higher activity than Au/Al_2O_3 and Au/C catalysts. We could note that the mean particle sizes used in this work did not correspond to the sizes showing the highest activity of gold; hence, the authors needed to use high temperatures. This led to low selectivity for hydrogen production, since high temperatures favour reverse WGS reaction giving CO and water from CO_2 and hydrogen over some of the catalysts. Also, in accordance with the results of our studies for an Au/TiO_2 catalyst,[10] Gazsi *et al.*[9] showed that the selectivity could be significantly improved with addition of water vapour to the reaction mixture. In contrast, addition of CO did not influence hydrogen production from formic acid[6,10] as CO is known not to be adsorbed strongly on any Au species.

Catalytic reactions on Au nanoparticles are very sensitive to the nature of the support;[11–14] however, explanations for these effects are contradictory and demand further studies. Hence, the objective of the present work was to reveal the effect of the nature of the oxide support in hydrogen production *via* formic acid decomposition for gold catalysts. We showed that the catalytic activity of the catalysts with the same mean metal particle sizes (2.4–3.0 nm) is strongly dependent on the acidity of the support. The Au/Al_2O_3 catalyst possessed the best performance in the reaction followed by Au/ZrO_2, Au/CeO_2, Au/La_2O_3 and Au/MgO catalysts.

Experimental

Materials

The catalyst supports and catalysts used in this work have been described earlier by us.[13] The following oxides have been used as supports: CeO_2, γ-Al_2O_3, La_2O_3, ZrO_2 (all from Alfa Aesar) and MgO (Mallinckrodt). According to XRD studies, ZrO_2 possessed a monoclinic structure, La_2O_3 a hexagonal one, while CeO_2, γ-Al_2O_3 and MgO demonstrated cubic structures. Au catalysts supported on different metal oxides were synthesized by a deposition–precipitation technique using $HAuCl_4$ (Alfa Aesar) as a metal precursor and urea as a precipitating agent to yield 3 wt% of Au as proposed by Zanella *et al.*[15] The prepared materials were washed with concentrated NH_4OH (25 M) to remove chlorides after gold deposition. This treatment was also important to clean the catalysts from other impurities, like alkali metal ions. Then, the samples were washed with distilled water, filtered and dried for 24 h at room temperature. These samples were denoted as initial. The samples denoted as calcined were heated in oxygen from room temperature up to 623 K with a ramp of 20 K min^{-1} and were immediately cooled back to room temperature. The sample denoted as reduced was heated in H_2 up to 573 K and cooled rapidly to room temperature.

Catalyst characterization

The content of Au in the obtained gold catalysts was measured by inductively coupled plasma atomic emission spectroscopy (ICPAES) using a Varian Liberty 110 spectrometer.

A conventional JEOL JEM-2010 microscope was used for TEM imaging of the calcined Au catalysts supported on different metal oxides before the reaction. Additionally, the calcined Au/Al_2O_3 catalyst was studied after the formic acid decomposition using a Titan 60–300 TEM/STEM microscope (FEI, Netherlands) in HAADF/STEM mode. The samples for this analysis were prepared by ultrasound dispersion in isopropanol and a drop of the solution was put on a carbon grid.

The electronic state of gold species was studied by X-ray photoelectron spectroscopy (XPS) with a Kratos AXIS 165 photoelectron spectrometer using monochromatic AlKα radiation ($h\nu$ = 1486.58 eV). All measured binding energies were referred to the C 1s line of carbon at 284.8 eV.

The Au-L_3 edge EXAFS spectra of the Au/Al_2O_3 catalyst were measured at the Siberian Synchrotron and Terahertz Radiation Centre (SSTRC, Novosibirsk, Russia). The storage ring VEPP-3 with an electron beam energy of 2 GeV and an average stored current of 90 mA was used as a source of radiation. The X-ray energy was monitored with a channel cut Si(111) monochromator. Harmonic rejection was performed by using a SiO_2 mirror for all measurements.

All EXAFS spectra were recorded under transmission and fluorescent mode with steps of 1.5 eV. Energy calibration was done using a gold foil spectrum. The spectra were treated using standard procedures.[16,17] The background was removed by extrapolating the pre-edge region onto the EXAFS region in the form of polynomials. Three cubic splines were used to construct the smooth part of the absorption coefficient. The inflection point of the edge of the X-ray absorption spectrum was used as the initial point (k = 0) of the EXAFS spectrum. The radial distribution function of atoms (RDF) was calculated from the spectra in $k^3\chi(k)$ by using Fourier transform modulus in the wavenumber interval of 3.0–12.0 $Å^{-1}$.

A curve fitting procedure with Viper[17] and EXCURV92[18] codes was applied to determine the distances and coordination numbers. It was performed for $k^3\chi(k)$ in similar wavenumber intervals after preliminary Fourier filtering by using the known XRD literature data for the bulk compounds. The Debye–Waller factors were fixed: $2\sigma^2$ = 0.009–0.013 $Å^2$.

Catalytic activity measurements

Vapour phase formic acid decomposition was carried out in a fixed bed quartz reactor with 4 mm internal diameter under normal atmospheric pressure as was described earlier.[19] The loading of a catalyst was 23.5 mg and it was placed between

two layers of quartz wool. The catalytic activities were measured after the reduction of the catalysts in a 1 vol% H_2/Ar mixture for 1 h at 573 K followed by cooling in He to the reaction temperature.

Formic acid (Sigma-Aldrich) was introduced into an evaporator by a syringe-pump (Sage) to get 1.9 vol% in helium flow. The total flow rate of the gas mixture was 51 mL min^{-1} for all experiments. A gas chromatograph (HP-5890) equipped with a thermal conductivity detector and a Porapak-Q column was used for gas analysis. To evaluate the temperature dependence of the acid conversion, the composition of the outlet gas mixture was measured several times at each temperature (at least for 30 min), to ensure that the activity was stable in time. As there was only negligible content of other carbon-containing products apart from CO and CO_2, the degree of conversion of formic acid was determined as the sum of CO and CO_2 concentrations related to the initial concentration of formic acid. Apparent activation energies and turnover frequencies (TOFs) were calculated at low conversions (<20%). The TOFs were determined based on the total number of metal atoms in the sample.

Results

Characterization of the catalysts and supports

Table 1 shows some characterization data for the calcined Au catalysts on different supports studied. It is seen that the BET surface areas of the supports differed from 2 to 136 $m^2\ g^{-1}$. In spite of this, the average pore diameters were quite similar ranging from 4.0 to 6.6 nm. These sizes indicate that the catalysts were mainly mesoporous implying easy transport of formic acid and products in the pores.

It is seen in Table 1 that the measured content of Au was slightly lower than the calculated one (3 wt%). This could be explained by a higher content of water in the Au precursor than expected. The mean Au particle sizes measured by conventional TEM (JEM-2010) were in the narrow range from 2.4 to 3.0 nm for all the catalysts studied. These particle sizes corresponded to the dispersion of 39–49% calculated for a spherical shape of the Au particles. As the difference in these values was small, we accepted that the mean particle size was the same for all samples. This approach facilitated substantially the elucidation of the support effect for the reaction allowing the particle size effect to be neglected.

Table 1 BET surfaces areas (S_{BET}), average pore diameters, Au content, mean Au particle sizes determined by TEM and apparent activation energies for formic acid decomposition (E_a) for the calcined catalysts

Catalysts	S_{BET}, $m^2\ g^{-1}$	Average pore diameter in metal oxide, nm	Au content, wt%	Mean Au particle size, nm	E_a, kJ mol^{-1}
Au/Al_2O_3	136	5.4	2.50	2.6	57
Au/ZrO_2	110	6.6	2.57	2.5	53
Au/MgO	105	4.0	2.59	3.0	44
Au/CeO_2	14	6.0	2.59	2.4	39
Au/La_2O_3	2	5.7	2.06	2.4	56

Based on the earlier studies,[5–7] one can suppose that some catalyst supports may provide stabilization of sub-nanometre sized Au species in the form of isolated atoms in a cationic state. Hence, we used EXAFS, XPS and HAADF/STEM to reveal the state of Au in the most active Au/Al_2O_3 sample.

EXAFS spectroscopy is a well-known powerful instrument which allows direct information concerning the local arrangement of gold in nanosized (nanostructured) systems to be obtained.[20] The interatomic distances (R) and coordination numbers (CN) are the main parameters, which can be estimated by this method. Earlier, we have studied different gold mono- and hetero-metallic nanosystems, including nanostructured catalysts stabilized on oxide supports by means of EXAFS, and showed that this method is useful for structural studies and phase analysis of active components for highly dispersed and low-metal content catalysts.[21,22]

The curves of the radial distribution function of atoms (RDF) describing the local arrangement of gold for the initial and reduced Au/Al_2O_3 samples are shown in Fig. 1. The initial sample is the sample obtained after the deposition of Au species, their hydrolysis and drying at room temperature. This sample was not calcined at high temperatures and was not reduced. A comparison of the curves was performed with the curves obtained for the reference Au foil. For the initial sample, no metallic Au^0 species were determined within the method limit. Obviously, the first main peak in RDF located at 1.2–2.2 Å must be attributed to the Au–O distance ~2.0 Å,[23,24] while the next two low amplitude peaks within the region 2.3–4.0 Å – to a few Au–O–Au distances. Fitting gives the following set of values: R_{Au-O} ~ 1.98 Å, CN ~ 5.9-6.0; $R_{Au-O-Au}$ ~ 3.05 Å, CN ~ 2.2; $R_{Au-O-Au}$ = 3.69–3.74 Å, CN ~ 2.3 (Table 2). These Au parameters correspond to a hydroxy-oxide structure, which is not similar to that of the bulk Au_2O_3 oxide

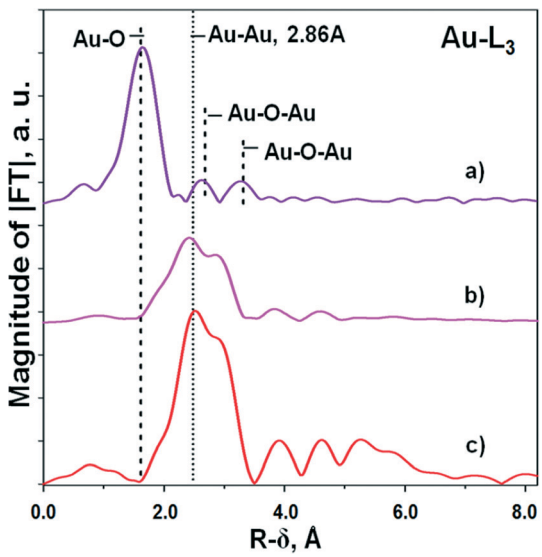

Fig. 1 The curves of the radial distribution function of atoms (RDF) describing the local arrangement of gold for the a) initial unreduced Au/Al_2O_3 catalyst, b) reduced Au/Al_2O_3 catalyst and c) Au foil – reference sample.

Table 2 Structural data calculated from EXAFS (Au-L_3) spectra (R – distances and CN – coordination numbers) of the studied samples

	Au/Al_2O_3, initial		Au/Al_2O_3, reduced		Au foil	
	R, Å	CN	R, Å	CN	R, Å	CN
Au–O	1.98	5.9–6.0	—	—	—	—
Au–Au	—	—	2.81	6.4–6.9	2.86	12.0
Au–O–Au	3.05	2.2	—	—	—	—
Au–O–Au	3.69–3.74	2.3	—	—	—	—

(Au^{3+} cations in 4-coordinated positions),[23] because Au^{3+} cations are located in almost octahedral oxygen surrounding.

In contrast, the reduced sample contains only metallic species as no Au–O features were observed. The very high dispersion of Au observed from the TEM measurements (Table 1) is further confirmed by calculations of the shortest average distance between Au atoms and coordination number giving the values of ~2.81 Å and 6.4–6.9, respectively, in comparison with those values for the Au foil (2.86 Å and 12.0)[25] (Table 2). Very similar values were also obtained for the calcined sample.

XPS measurements of the calcined and reduced Au/Al_2O_3 catalysts led to very similar spectra with binding energies for the Au 4f doublet at 83.9 and 87.6 eV, indicating the presence of metallic Au (Fig. 2). One can suppose the presence of shoulders for these lines at about 5% of the intensity located at higher binding energy tails of the peaks, which could be related to $Au^{\delta+}$ species. However, as the shoulders do not change with high temperature reduction, the possibility of the presence of these species is low.

The mean particle size for the calcined Au/Al_2O_3 sample after the reaction measured with atomic resolution HAADF/STEM (Titan 60–300, Fig. 3a) was the same as before the reaction measured by conventional TEM (Table 1). This indicated that the reaction does not influence significantly the size of the Au nanoparticles.

The major aim for utilization of HAADF/STEM was to reveal the presence of small clusters and isolated Au species.

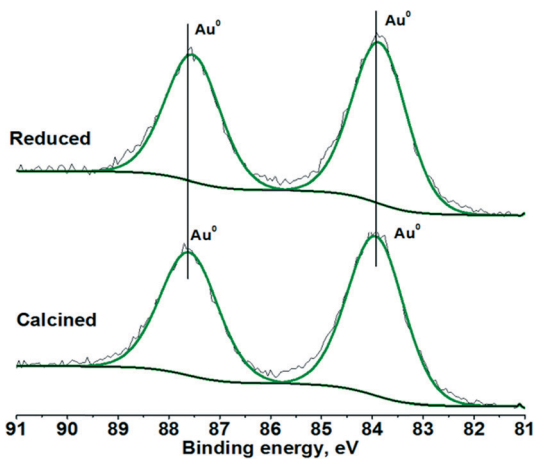

Fig. 2 Au 4f XPS spectra of the calcined and reduced Au/Al_2O_3 catalysts.

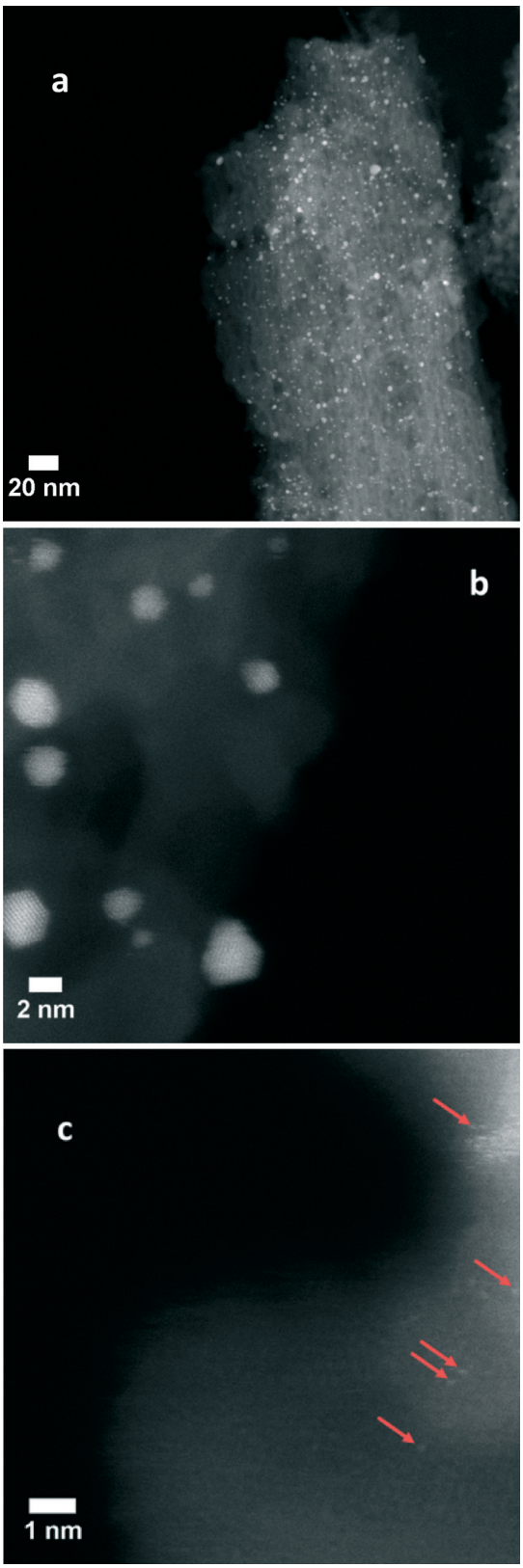

Fig. 3 Low (a) and high (b, c) resolution HAADF/STEM images of the calcined Au/Al_2O_3 catalyst after the reaction (single atoms are indicated with arrows).

Earlier, this approach allowed us to reveal a large content of isolated Pd atoms in Pd catalysts supported on nitrogen-doped mesoporous carbon.[19] Using a number of methods and DFT calculations, we showed that these species could be the active sites for formic acid decomposition. In the present work, the images of the Au/Al_2O_3 catalyst depicted in Fig. 3b and c demonstrate that very rare small clusters and isolated atoms could be seen in the sample. It was really difficult to find them, as their content was too small in comparison with the content of larger Au nanoparticles. Moreover, we cannot conclude definitively that all the observed single atoms are Au and not some impurities in the sample.

Catalytic properties of the catalysts on different supports

The catalytic activity for the calcined Au catalysts on different supports was compared at high conversions by comparing the temperatures for 50% conversion (Fig. 4a) as well as at small conversions by comparing the TOF values (Fig. 5). It is seen in Fig. 4a that the Au/Al_2O_3 catalyst showed the lowest temperature for 50% conversion. It was followed by the Au/La_2O_3 and Au/ZrO_2 catalysts, while the catalysts on the MgO and CeO_2 supports were much less active. The selectivity for hydrogen production was also the highest for the Au/Al_2O_3 catalyst (Fig. 4b). The lowest selectivity of about 90% was

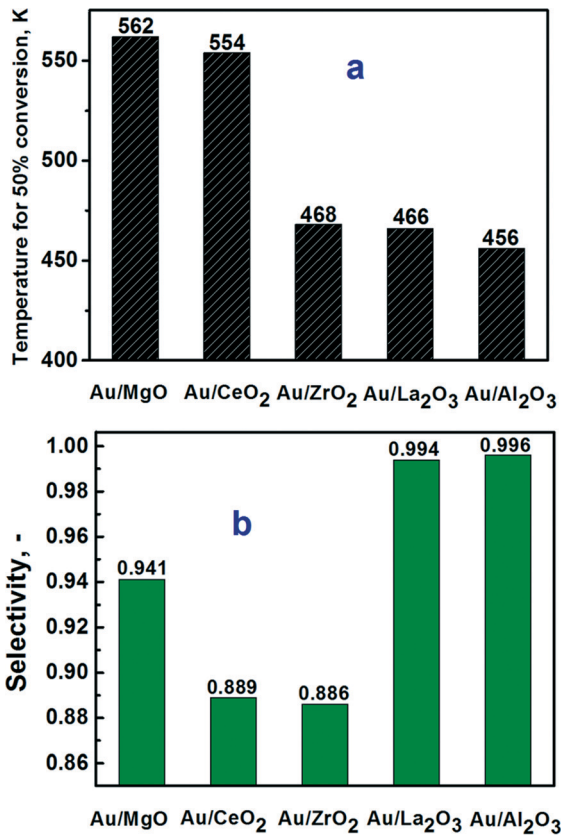

Fig. 4 a) Temperature for 50% of conversion of formic acid and b) selectivity to hydrogen at this temperature for the calcined Au catalysts supported on different metal oxides.

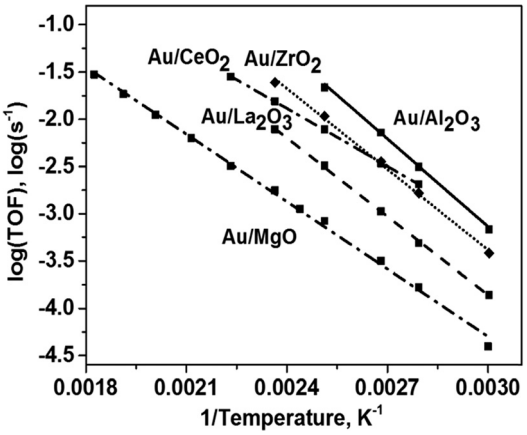

Fig. 5 Arrhenius plots for TOFs in the decomposition of formic acid on the calcined Au catalysts supported on different metal oxides.

obtained for the Au/CeO_2 and Au/ZrO_2 catalysts. These catalysts were probably very active in reverse WGS reaction converting H_2 and CO_2 products to CO and H_2O.

The Arrhenius plots for the TOFs for formic acid conversion over the Au catalysts on different supports are shown in Fig. 5. The activity trend of the catalysts differed slightly from the trend obtained at 50% conversion (Fig. 4a). However, the Au/Al_2O_3 catalyst was still the most active catalyst and the Au/MgO catalyst possessed the lowest activity. At the same time, this Au/MgO catalyst was highly active in liquid phase oxidation of alcohols.[21] The apparent activation energies for formic acid decomposition (Table 1) were quite similar for the Au catalysts on the Al_2O_3, ZrO_2 and La_2O_3 supports, showing the values of 53–57 kJ mol^{-1}, while the values were lower for the catalysts supported on MgO and CeO_2 – 44 and 39 kJ mol^{-1}, respectively.

Using an approach applied in ref. 12 and 13, we plotted the TOFs as a function of the electronegativity of the support's cation (X_i). The latter value was calculated from Pauling's electronegativity (x_0) and the charge of the metal cation (Z) using an equation ($X_i = (1 + 2Z)^*x_0$).[26] The TOFs at 373 K plotted as a function of the electronegativity of the metal cation demonstrated a strong volcano-type dependence with the Au/Al_2O_3 catalyst on the top (Fig. 6a). It is evident that for the optimal performance, the support should not be too basic as the activity of the most basic Au/MgO catalyst was about 20 times lower than that of the Au/Al_2O_3 catalyst. The Au/Al_2O_3 catalyst showed almost CO-free hydrogen production. The CO content was less than 40 ppm under these conditions (Fig. 6b), whereas the others showed a higher content of CO in the products. There is also an important question whether the Au/Al_2O_3 catalyst can be stable in the reaction for a long time. The result of long-term testing of the reduced sample is shown in Fig. 7. It is seen that the conversion of formic acid over this catalyst changes only weakly from 61 to 55% within 16 h. The low content of CO and good stability could be important for possible utilization of the catalyst in fuel cells.

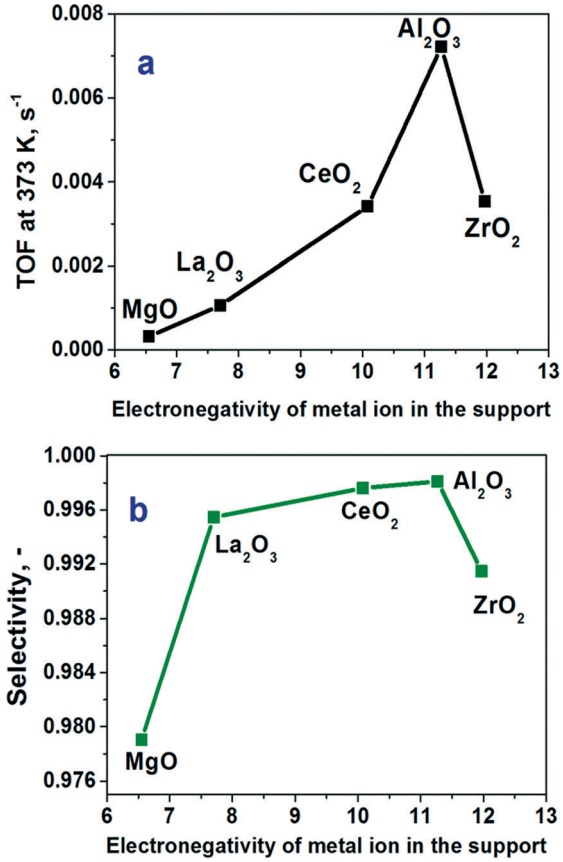

Fig. 6 Relationships between the a) TOFs and b) selectivity to hydrogen in formic acid decomposition over the calcined Au catalysts at 373 K on the electronegativity of metal ions of the used metal oxide supports.

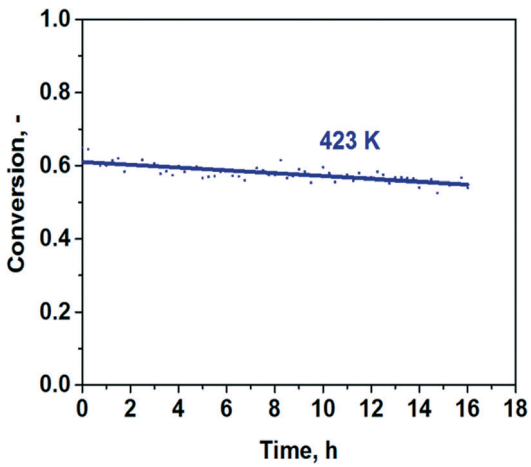

Fig. 7 Long-term stability test with the reduced Au/Al_2O_3 sample at 423 K.

Discussion

As we showed above, the comparison of the performances of the catalysts on different supports with the same mean Au particle sizes led to a conclusion that the Au/Al_2O_3 catalyst possesses the best performance with the highest activity and selectivity for hydrogen production. This catalyst also demonstrated a sufficient stability. Earlier, the superior activity of highly dispersed Au[11,27] and Ag[28] catalysts on alumina supports as compared to the catalysts on other supports has been reported for different reactions. The dependence of the TOFs on the electronegativity of the metal cation in the support clearly points out that the activity depends on the ability of the cation to withdraw electrons. This determines the acid–base properties of the support and indicates that these properties influence strongly the activity of the Au catalysts.

It is interesting that the observed trend of the activity corresponds well to the trend of the content of Lewis acid sites in the same supports, which we measured earlier by pyridine adsorption combined with FTIR spectroscopy.[14] The alumina support possessed the highest content of Lewis acid sites (25 $\mu mol\ g^{-1}$), while CeO_2 and ZrO_2 contained a lower concentration of these sites (10 $\mu mol\ g^{-1}$ for both), which were stronger for CeO_2. The MgO and La_2O_3 supports did not show any presence of Lewis acid sites able to adsorb pyridine. These data indicate that the Lewis acid sites are important for the activation of formic acid. Additionally, the basic supports (MgO, La_2O_3) adsorb strongly the product of the reaction (CO_2) leading to the poisoning of the support surface at low temperatures used.

It could be useful to compare the rates of the reaction over the catalysts and catalyst supports. The results for formic acid decomposition over oxide materials have been reviewed by Trillo *et al.*[29] They showed that oxides like Al_2O_3, MgO, TiO_2 and others are less active in the reaction as the decomposition takes place at much higher temperatures (>550 K) as compared to that over the studied supported Au catalysts (>373 K). In a more recent study, Patermarakis[30] has studied the kinetics of formic acid decomposition over γ-Al_2O_3 with a BET surface area close to our Al_2O_3 support. Formic acid dehydration was the major path of the conversion of formic acid with an apparent activation energy of about 87 kJ mol^{-1} and about 130 kJ mol^{-1} for dehydrogenation. Both values were much higher than that for the Au/Al_2O_3 catalyst (57 kJ mol^{-1}, Table 1). The rate of formic acid conversion over Al_2O_3 at 373 K estimated from the data of Patermarakis was by 3 orders of magnitude lower than that over our Au/Al_2O_3 catalyst. Hence, the direct contribution of the reaction over the support is negligible.

It is interesting that the CeO_2 and ZrO_2 supports as compared to the others are reducible oxide supports; however, this fact is not predominant for the catalytic activity in the considered reaction. As the Al_2O_3 support is amphoteric and contains both types of sites: acidic and basic, they both could play a certain role in formic acid conversion. For example, as proposed by Shimizu *et al.*[28] basic sites may facilitate the abstracting of proton from alcohol forming an alkoxide intermediate, while acidic sites ($OH^{\delta+}$) facilitate hydrogen transfer.

We consider several possible reasons for the explanation of the highest activity of the Au/Al_2O_3 catalyst in hydrogen production from formic acid as compared to the catalysts

with the same mean Au particle size on the other supports (Fig. 6a). Among them, we can mention the highest concentration of single Au atoms/cations as possible active sites, the optimized electronic properties or the shape of Au nanoparticles on the alumina support and the highest concentration of reaction intermediates formed on the support further transforming on the Au/alumina interface to the reaction products. The analysis of the surface of the Au/Al_2O_3 sample by XPS, and of the bulk by EXAFS and HAADF/STEM indicated the presence of only metallic Au nanoparticles. Therefore, we cannot accept that the support effect is related to a higher concentration of Au atoms/cations on the Al_2O_3 support than on the other supports; however, further experiments with catalysts leached by NaCN could be useful to determine the content of Au ions quantitatively. The electronic properties of Au in the catalysts on the same supports were analysed earlier by XPS and no serious change in the position of the Au 4f peak was observed.[13] Hence, we cannot assign the difference in the activity of Au on the nature of the support to the difference in electronic properties of the Au nanoparticles. We cannot also accept the approach related to the different contents of some specific sites, for example, corner sites in the Au nanoparticles on different supports, as we do not expect a strong dependence of the shape of Au nanoparticles on the acidity of the support with an optimum for the alumina. Moreover, as we reported earlier, the shapes of the Au particles on some supports were quite similar.[13]

Therefore, the observed behaviour of the catalytic activity should be attributed to the activation of the formic acid molecule on the support sites followed by further conversion of the formed reaction intermediate on some interfacial corner or edge sites of Au nanoparticles[8,31] giving hydrogen and carbon dioxide. The role of interfacial sites is considered for a number of catalytic reactions including CO oxidation and H_2/D_2 exchange.[32] An FTIR study could be useful to determine the nature of the intermediate. However, it will not be easy to do this, as for example, the nature of the intermediate for the WGS reaction is still under discussion. Thus, formate or carboxyl species are considered by different authors.[33] The problem is that formic acid should interact strongly with the support forming surface formate species, a significant part of which does not possess reaction ability.[33,34]

It could be also of interest to compare the activity of the Au/Al_2O_3 catalyst and the apparent activation energies with the literature data. The obtained apparent activation energy values of 57 kJ mol^{-1} corresponded well to the literature data for different Au catalysts,[4,6,9,10,35] not only limited to the catalysts with single supported Au atoms as active sites.[4,6] At the same time, the analysis showed that the TOFs obtained in our work were lower than those obtained for the catalysts with single Au atomic species. However, we expect that the activity of the catalysts could be significantly improved by using alkali metal ions as promoters. We showed earlier that the application of potassium carbonate/formate as a promoter improved the reaction rate over a Pd/C catalyst containing nanoparticles of about 3.6 nm by 1–2 orders of magnitude and this takes place because of a change in the mechanism of the reaction.[36,37]

Conclusions

The Au/Al_2O_3 catalyst showed the highest activity and almost CO-free hydrogen production in formic acid decomposition in comparison with the Au catalysts with the same mean Au particle sizes (2.4–3.0 nm) on ZrO_2, CeO_2, La_2O_3 and MgO supports. After being plotted as a function of the electronegativity of the metal ion in the support, the TOF values showed a volcano-type curve indicating a dependence of the catalytic activity on the acid–base properties of the support. The major mechanism of the reaction, taking place on the studied catalysts, was related to the activation of formic acid on the catalyst's support followed by further conversion of the formed intermediate on metal/support interface sites.

Acknowledgements

This publication has emanated from research conducted with the financial support of the Russian Science Foundation (Grant 16-13-00016). Collaboration between partner institutions was partly supported by European FP7 IRSES project 295180 (MagNonMag) as well as by CONACyT (México) and PAPIIT-UNAM (México) through Grants 179619 and 203813, respectively. The work related to the measurements of EXAFS spectra was supported by RFBR (14-03-01066, 16-03-01139). It was done using the infrastructure of the Shared-Use Centre "Siberian Synchrotron and Terahertz Radiation Centre" based on VEPP-3M of BINP SB RAS. M. Z. acknowledges the support of the Earth and Natural Sciences Doctoral Studies Programme, funded by the Higher Education Authority through the Programme of Research at Third Level Institutions, Cycle 5, co-funded by the European Regional Development Fund. A. L. C. acknowledges financial and technical support of FEI Company in the frame of collaboration project.

References

1 A. K. Singh, S. Singh and A. Kumar, *Catal. Sci. Technol.*, 2016, **6**, 12–40.
2 D. A. Bulushev and J. R. H. Ross, *Catal. Today*, 2011, **163**, 42–46.
3 J. C. Serrano-Ruiz, D. J. Braden, R. M. West and J. A. Dumesic, *Appl. Catal., B*, 2010, **100**, 184–189.
4 M. Ojeda and E. Iglesia, *Angew. Chem., Int. Ed.*, 2009, **48**, 4800–4803.
5 M. Flytzani-Stephanopoulos, *Accounts in Chemical Research*, 2014, vol. 47, pp. 783–792.
6 N. Yi, H. Saltsburg and M. Flytzani-Stephanopoulos, *ChemSusChem*, 2013, **6**, 816–819.
7 A. Ciftci, D. Ligthart, P. Pastorino and E. J. M. Hensen, *Appl. Catal., B*, 2013, **130**, 325–335.

8 S. Singh, S. Li, R. Carrasquillo-Flores, A. C. Alba-Rubio, J. A. Dumesic and M. Mavrikakis, *AIChE J.*, 2014, **60**, 1303–1319.
9 A. Gazsi, T. Bansagi and F. Solymosi, *J. Phys. Chem. C*, 2011, **115**, 15459–15466.
10 D. A. Bulushev, S. Beloshapkin and J. R. H. Ross, *Catal. Today*, 2010, **154**, 7–12.
11 G. A. Filonenko, W. L. Vrijburg, E. J. M. Hensen and E. A. Pidko, *J. Catal.*, DOI: 10.1016/j.jcat.2015.10.002.
12 T. Ishida, R. Takamura, T. Takei, T. Akita and M. Haruta, *Appl. Catal., A*, 2012, **413**, 261–266.
13 Y. S. Demidova, I. L. Simakova, M. Estrada, S. Beloshapkin, E. V. Suslov, D. V. Korchagina, K. P. Volcho, N. F. Salakhutdinov, A. V. Simakov and D. Y. Murzin, *Appl. Catal., A*, 2013, **464**, 348–356.
14 O. A. Simakova, E. Smolentseva, M. Estrada, E. V. Murzina, S. Beloshapkin, S. M. Willfor, A. V. Simakov and D. Y. Murzin, *J. Catal.*, 2012, **291**, 95–103.
15 R. Zanella, S. Giorgio, C. R. Henry and C. Louis, *J. Phys. Chem. B*, 2002, **106**, 7634–7642.
16 D. I. Kochubey, *EXAFS spectroscopy of catalysts*, Nauka, Novosibirsk, 1992.
17 K. V. Klementiev, *VIPER (Visual Processing in EXAFS Researches)*, https://intranet.cells.es/Beamlines/CLAESS/software/viper.html.
18 N. Binsted, J. V. Campbell, S. J. Gurman and P. C. Stephenson, *EXCURV92 program code*, SERC Daresbury Laboratory, Daresbury, 1991.
19 D. A. Bulushev, M. Zacharska, E. V. Shlyakhova, A. L. Chuvilin, Y. Guo, S. Beloshapkin, A. V. Okotrub and L. G. Bulusheva, *ACS Catal.*, 2016, **6**, 681–691.
20 D. C. Konigsberger and R. Prins, *X-ray absorption principles and application techniques*, Wiley, New York, 1988.
21 V. V. Costa, M. B. Estrada, Y. Demidova, I. Prosvirin, V. Kriventsov, R. F. Cotta, S. Fuentes, A. Simakov and E. V. Gusevskaya, *J. Catal.*, 2012, **292**, 148–156.
22 S. A. Nikolaev, A. V. Chistyakov, M. V. Chudakova, E. P. Yakimchuk, V. V. Kriventsov and M. V. Tsodikov, *J. Catal.*, 2013, **297**, 296–305.
23 ICSD Database Code 8014 -Au2O3.
24 ICSD Database Code 64701 -AuAlO2.
25 ICSD Database Code 64701 -Au^0.
26 K. Tanaka and A. Ozaki, *J. Catal.*, 1967, **8**, 1–7.
27 E. Smolentseva, A. Simakov, S. Beloshapkin, M. Estrada, E. Vargas, V. Sobolev, R. Kenzhin and S. Fuentes, *Appl. Catal., B*, 2012, **115**, 117–128.
28 K. Shimizu, M. Nishimura and A. Satsuma, *ChemCatChem*, 2009, **1**, 497–503.
29 J. M. Trillo, G. Munera and J. M. Criado, *Catal. Rev.*, 1972, **7**, 51–86.
30 G. Patermarakis, *Appl. Catal., A*, 2003, **252**, 231–241.
31 J. Ohyama, A. Esaki, T. Koketsu, Y. Yamamoto, S. Arai and A. Satsuma, *J. Catal.*, 2016, **335**, 24–35.
32 M. Haruta, *Angew. Chem., Int. Ed.*, 2014, **53**, 52–56.
33 R. Burch, A. Goguet and F. C. Meunier, *Appl. Catal., A*, 2011, **409**, 3–12.
34 C. M. Kalamaras, G. G. Olympiou and A. M. Efstathiou, *Catal. Today*, 2008, **138**, 228–234.
35 D. A. Bulushev, S. Beloshapkin, P. E. Plyusnin, Y. V. Shubin, V. I. Bukhtiyarov, S. V. Korenev and J. R. H. Ross, *J. Catal.*, 2013, **299**, 171–180.
36 L. Jia, D. A. Bulushev, S. Beloshapkin and J. R. H. Ross, *Appl. Catal., B*, 2014, **160**, 35–43.
37 L. Jia, D. A. Bulushev and J. R. H. Ross, *Catal. Today*, 2016, **259**, 453–459.